

LETTER • OPEN ACCESS

## A stimulated Stokes Raman scattering-based approach for continuous wave supercontinuum generation in optical fibers

To cite this article: Muhammad Assad Arshad *et al* 2019 *Laser Phys. Lett.* **16** 035108

View the [article online](#) for updates and enhancements.

### You may also like

- [Impact of refractive index mismatches on coherent anti-Stokes Raman scattering and multiphoton autofluorescence tomography of human skin \*in vivo\*](#)  
M Weinigel, H G Breunig, M E Darvin *et al.*
- [Thermometry in internal combustion engines via dual-broadband rotational coherent anti-Stokes Raman spectroscopy](#)  
C Brackmann, J Bood, M Afzelius *et al.*
- [Nanoscale nonlinear optics in photonic-crystal fibres](#)  
Alekssei Zheltikov

### Recent citations

- [Influences on the direction probabilities for the direction instability phenomenon in fiber ring lasers](#)  
M. A. Arshad *et al*



## IOP | ebooks™

Bringing together innovative digital publishing with leading authors from the global scientific community.

Start exploring the collection—download the first chapter of every title for free.

## Letter

# A stimulated Stokes Raman scattering-based approach for continuous wave supercontinuum generation in optical fibers

Muhammad Assad Arshad, Alexander Hartung and Matthias Jäger

Leibniz-Institute of Photonic Technology, Albert-Einstein-Straße 9, 07745 Jena, Germany

E-mail: [Muhammad.arshad@leibniz-ipht.de](mailto:Muhammad.arshad@leibniz-ipht.de)

Received 17 October 2018, revised 2 January 2019

Accepted for publication 3 January 2019

Published 8 February 2019



CrossMark

**Abstract**

We report on a new and simple approach for continuous wave supercontinuum generation in optical fibers. Our new approach uses the effect of stimulated Stokes Raman scattering in a low loss fiber ring laser. By continuously pumping this ring laser with up to 19 W optical power we excited up to six Stokes orders and covered a wavelength range of 500 nm. Due to the feedback mechanism of the ring layout additional nonlinear effects occurred next to the plain generation of individual Stokes peaks. Eventually, these effects broaden and merge the separated Stokes peaks and create a single, connected continuous supercontinuum. By using the effect of stimulated Stokes Raman scattering, we do not rely on anomalous dispersion and modulation instability as typically required for continuous wave supercontinuum generation.

Keywords: fiber ring laser, cascaded Stokes Raman scattering, continuous wave supercontinuum generation, nonlinear optics

(Some figures may appear in colour only in the online journal)

**1. Introduction**

Continuous wave (cw) supercontinuum (SC) generation is typically conducted using a simple setup comprising only a cw pump source and a suitable optical fiber [1]. The pump source is usually an Yb- or Er-doped fiber laser with a few tens of Watt output power. According to the pump source the optical fiber has to meet certain criteria. Most important criterion is the group velocity dispersion which has to be low and anomalous at the pump wavelength to utilize modulation instability which is the key to cw SC generation [2, 3]. This instability enables the decay of the cw envelope into pulses followed by the creation of optical solitons to initiate the

nonlinear processes required for efficient cw SC generation like soliton self-frequency shift [4, 5] and inter-soliton collision [6, 7].

For an Er-based pump wavelength around 1.5  $\mu\text{m}$  this dispersion requirement can be met with conventional dispersion shifted fibers or highly nonlinear fibers [8]. For pump wavelengths around 1  $\mu\text{m}$  this dispersion requirement is typically met with photonic crystal fibers (PCFs) [9]. The use of a PCF makes a low loss splice to the fiber laser quite challenging. In addition, since several tens of meters of fiber are required, this makes the setup quite expensive. Both constrains, the need for expensive PCFs as well as the challenge of low loss splices, are released by the alternative approach of cw SC generation using a pump wavelength around 1  $\mu\text{m}$  we present below.

One basis if our approach is the effect of stimulated Stokes Raman scattering [10, 11] which does not require a specific dispersion management of the optical fiber. Hence, the fiber can be optimized regarding compatibility to other fiber optic

 Original content from this work may be used under the terms of the [Creative Commons Attribution 3.0 licence](https://creativecommons.org/licenses/by/3.0/). Any further distribution of this work must maintain attribution to the author(s) and the title of the work, journal citation and DOI.

components in use and typically a simple step index fiber is good enough.

The second basis is the ring cavity layout that enables a nonlinear feedback mechanism. While a single pass of the laser signal through the passive fiber results in a cascaded stimulated Stokes Raman scattering spectrum with well-separated Stokes peaks, the strong feedback of the ring layout triggers a multitude of additional nonlinear effects which finally connect the individual Stokes peaks to a single SC.

This manuscript is structured as follows. In section 2 we present the experimental setup and explain in detail the spectral properties of critical components. On section 3 we detail our experimental findings by comparing the spectral properties and power properties we obtain for different cavity layouts. Section 4 summaries and concludes the paper.

## 2. Setup and methods

The setup consists of an all-fiber ring cavity as shown in figure 1. The main intention of this simple setup is to effectively trigger nonlinear effects and get an at most broadband emission for a given pump power. In addition, the all-fiber design assures a preferably high power handling compared to alternative designs which include free space to fiber couplings as required when using an optical isolator. For small roundtrip losses the effect of cavity enhancement is also possible with our cavity design.

The cavity is pumped by a pump diode emitting at a wavelength of 976 nm up to a maximum of 19 W. The emitted pump power and hence the power circulating in the cavity is adjusted by varying the pump diode's supply current. The pump power enters the ring cavity by a pump signal combiner and reaches a 13 m long Yb-doped active fiber section (Nufern SM-YDF-5/130). Here, without any wavelength selective filter applied, a laser signal at around 1100 nm is emitted.

The active fiber is followed by 1 km or 2 km passive fiber (Corning HI1060) with a zero dispersion wavelength around 1400 nm. Finally, an output coupler (Gooch&Housego FFS-060N72X10; nominal coupling ratio is 0.01% at 1060 nm) feeds part of the signal back to the pump signal combiner where it passes through the ring again, and part of the signal out of the cavity. As no optical isolator is included in the ring cavity clockwise and counter clockwise signals are allowed to propagate. To minimize roundtrip losses similar mode field diameters in the range of 6.1  $\mu\text{m}$  to 6.6  $\mu\text{m}$  and only single mode components were selected. All components are non-polarization maintaining.

The spectral distribution of the generated SC is strongly co-determined by the wavelengths dependence of the propagation loss of the passive fiber and of the output coupler coupling ratio. The wavelength dependence of the propagation loss of the passive fiber is shown in figure 2. The fiber exhibits two O–H bonds related absorption peaks around 1250 nm and 1380 nm which cause spectral gaps in the SC as we will see later. In addition, losses strongly increase above 1700 nm due to bending in combination with the weak guidance far above the cutoff wavelength of 920 nm.

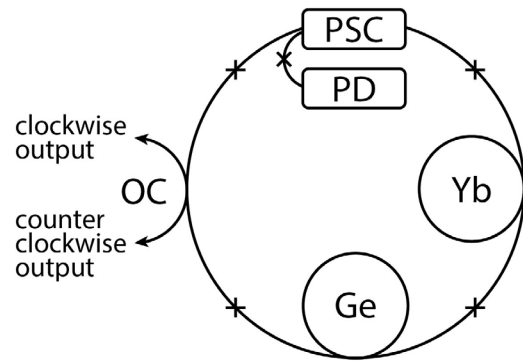


**Figure 1.** Scheme of the all-fiber ring laser. The setup consists of a pump diode (PD), a pump signal combiner (PSC), an active fiber (Yb), a passive fiber (Ge), and an output coupler (OC). Crosses represent fusion splices.

Figure 3 shows the wavelength dependence of the coupling ratio of the used output coupler (purple line, right y-axis). The coupling ratio is quite low around 0.01% at the ytterbium emission wavelengths, increases monotonously through the entire generated SC and approaches 50% at its long wavelength end near 1600 nm. Throughout the paper the coupler is used in both configurations providing firstly a low output coupling fraction of nominal 0.01% and secondly a high output coupling fraction of nominal 99.99%.

The SC spectra were measured using an ANDO AQ6317 spectrum. The output power was measured separately using a Thorlabs PM100D power meter. As the intracavity power cannot be measured directly it was determined by the following procedure: (a) normalizing the analyzer spectrum by the measured output power; (b) applying wavelength-by-wavelength the output couplers coupling ratio to the normalized output spectrum to calculate the intracavity spectrum; and (c) integrating the intracavity spectrum to calculate the intracavity power.

## 3. Results

In a first configuration we realized a cavity with a passive fiber length of 1 km and low output coupling ratio. The extracted SC at maximum pump power is shown in figure 3 (black line). The SC starts at 1070 nm and ends with its last strong Stokes peak around 1560 nm wavelength, albeit additional low intensity components are visible up to the analyzers operation limit at 1700 nm.

The envelope of the output spectrum follows quite closely the shape of the output coupling ratio (figure 3, purple line). For the intracavity distribution this means a similar—within one order of magnitude—power level for all propagating wavelengths component as demonstrated in figure 3, as well (gray line).

From a practical perspective, this offers the opportunity to emphasize specific spectral regions with a proper coupling profile of the output coupler while keeping unrequired wavelengths and optical power in the ring cavity for strengthening the nonlinear effects. Alternatively, wavelength independent couplers (WICs) can be used to flatten the output spectrum.

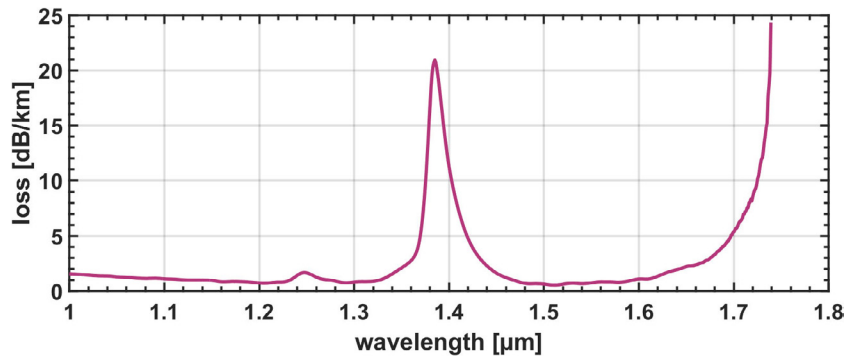


**Figure 2.** Loss profile of the Corning HI1060 (Raman active) fiber. Strong absorption peaks related to a high amount of O–H bonds are visible at 1250 nm and 1380 nm.

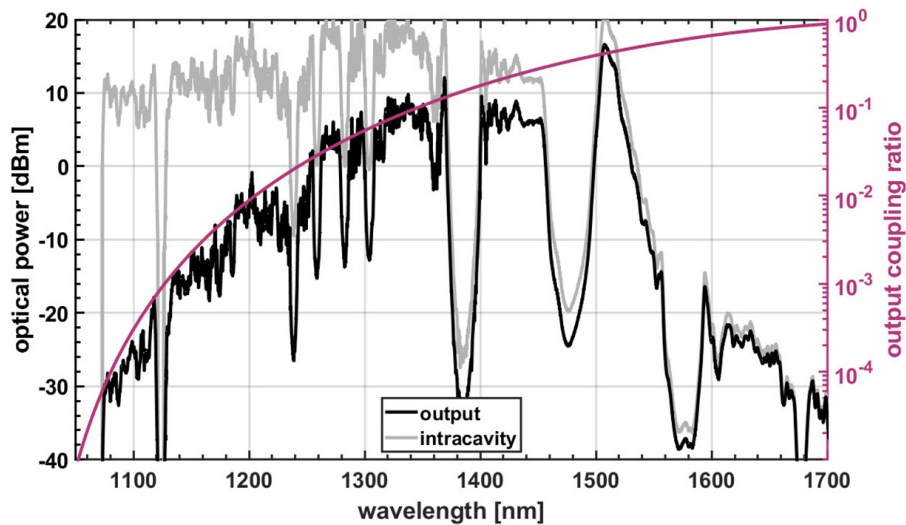


**Figure 3.** Output spectrum (black) for the first ring cavity with low output coupling ratio at maximum pump power of 19 W in comparison to the intracavity spectrum (gray) and the output coupling ratio (purple). Both y-axes are in logarithmic scale.

There are a few spectral gaps visible in the SC presented in figure 3, two of which, at 1240 nm and 1380 nm, can directly be related to the two O–H absorption bands of the 1 km long passive fiber shown in figure 2. We expect these gaps to be mitigated and eliminated by using a dry fiber with much less water content.

The spectral gap of the very strong absorption peak at 1380 nm also appears to cause the 13 THz red-shifted spectral gap around 1470 nm by preventing stimulated Stokes Raman scattering in this region. Thus, utilizing a low water fiber not only benefits the very absorption bands but additional spectral regions as well.

Figure 4 shows the evolution of the intracavity spectrum as a function of pump power. Clearly visible are the laser peak around 1100 nm and the six stimulated Stokes peaks as they emerge one by one from the noise floor. While they are quite narrow and distinguished from the existing spectrum at the moment of appearance they broaden quite fast and merge with other spectral components. This finally leads to a broad and mostly connected SC.

The spectral gap at 1380 nm caused by the loss profile of the fiber is also clearly visible. We expect the 1380 nm loss peak to be the main reason, why the 5th Stokes peak remains separated from the earlier ones and, due to suppressed stimulated

Raman scattering around 1470 nm, why the 6th Stokes peak remains separated, as well.

The merging of the individual Stokes peaks for this first, low output coupling layout is caused by the high internal power and does not occur for a second layout with high output coupling as shown in figures 5(a) and (b). Figure 5 shows in (a) the generated spectrum at maximum pump power and in (b) the spectral evolution for a second experimental configuration where we flipped the output coupler compared to the first configuration. Here, we have a nominal output coupling ratio of 99.99% resulting in an effectively linear cavity. In this case, the 4% Fresnel reflection at the accessible fiber ends of the coupler constitute the cavity mirrors.

There are a couple of noteworthy differences in the generated spectrum between the first and the second cavity layout. As already mentioned, the first, low output coupling layout leads to a considerable broadening and finally merging of the Stokes peaks only separated by the loss peak of the fiber, while the second, high output coupling layout keeps all the Stokes peaks separated. In addition, stimulated Stokes Raman scattering is strongly shifted to smaller powers for the first, low output coupling cavity. In this case, the first Stokes peak is generated already around 1.4 W pump power shortly after stimulated emission starts around 0.8 W. For the second,

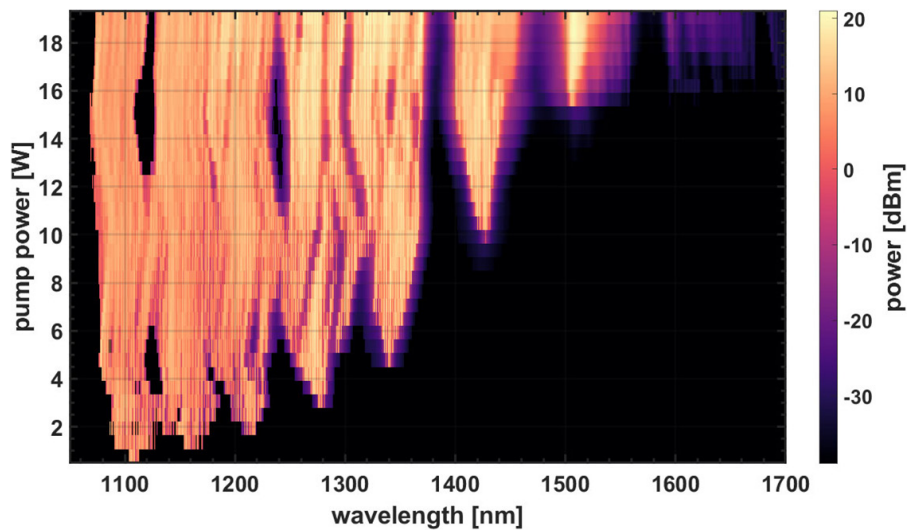


**Figure 4.** Spectral evolution as a function of pump power for the first ring cavity with low output coupling ratio. Stimulated Raman scattering occurs up to the 6th Stokes order.

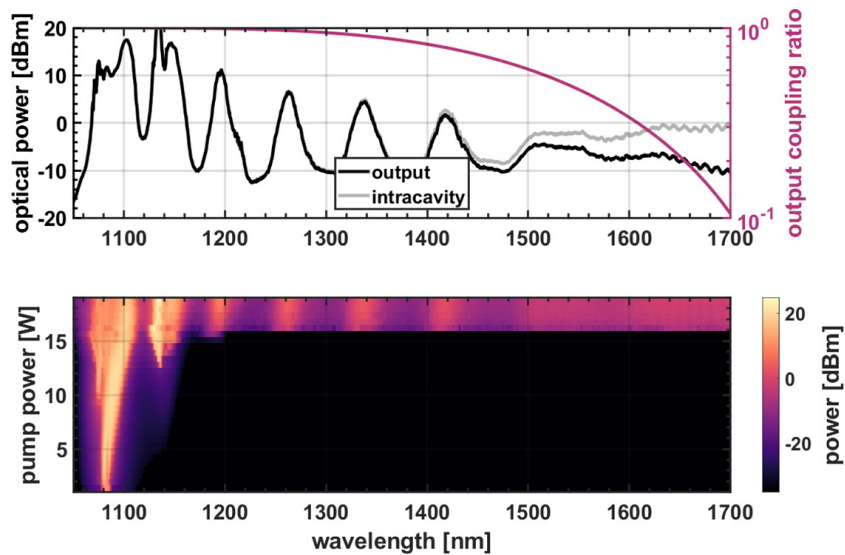


**Figure 5.** (a) Output spectrum at maximum pump power and (b) spectral evolution for the second ring cavity with a high output coupling fraction of nominal 99.99%.

effectively linear cavity the generation of the first Stokes peak shifts to a higher power value (12.8 W). Interestingly, shortly thereafter around 16.2 W numerous new wavelengths are generated in a single instant covering the entire remaining spectral range of the analyzer.

The evolution of the output power and the intracavity power as a function of the pump power for the first, low output coupling layout is shown in figure 6. Both, output power as well as intracavity power increase with the pump power. Due to the very low output coupling only a small amount of power is coupled out starting below 1% and reaching a maximum of 12% at maximum generated power as seen by the purple line in figure 4. This increasing output coupling efficiency is caused by the increasing amount of long wavelength components in combination with the output coupling ratio of the coupler that strongly increases towards longer wavelengths. Note, that the values stated in figure 6 correspond to a single propagation direction. Since there is no optical isolator used

in our setup the laser emits light equally in both directions and a similar power exits both accessible ends of the output coupler.

In a third cavity layout we extended the length of the Raman active fiber from 1 km to 2 km while maintaining the low output coupling fraction. This led to the surprising effect of unidirectional lasing and optical bistability [12] without using an optical Farady isolator [13] as demonstrated in figure 7. While increasing the pump power the combined output power of both propagation directions (figure 7(a)) exhibits besides an initial monotonic growth a sudden increase of ca. 60% near a pump power of 16.5 W. While decreasing the pump power this elevated output power level persists far below this initial switching power down to a pump power of 13.3 W where the system drops back to the same lower power observed during the power increase. In sum the system features a hysteresis with a high and a low output power level between two distinct switching points, hence optical bistability.

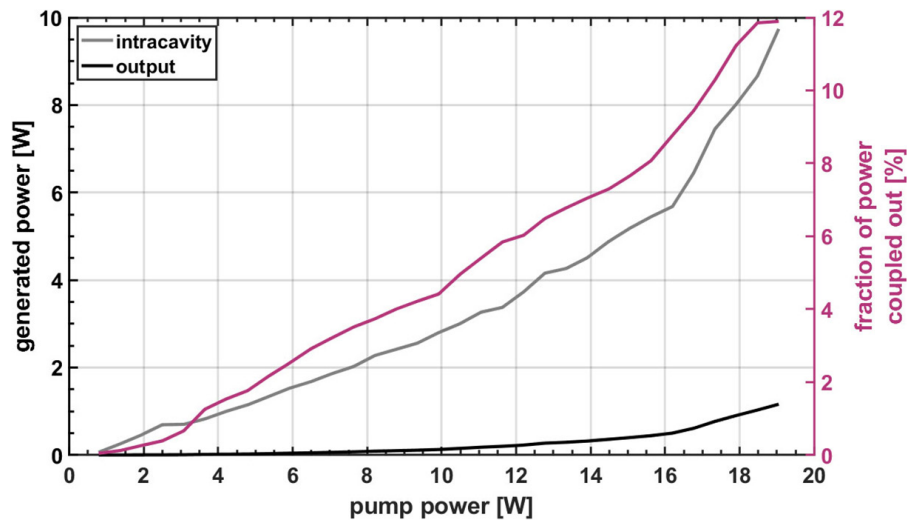


**Figure 6.** Generated power as a function of pump power for the first ring cavity with low output coupling fraction and 1 km passive fiber. Power values correspond to a single propagation direction. A similar amount of power travels in the opposite direction.

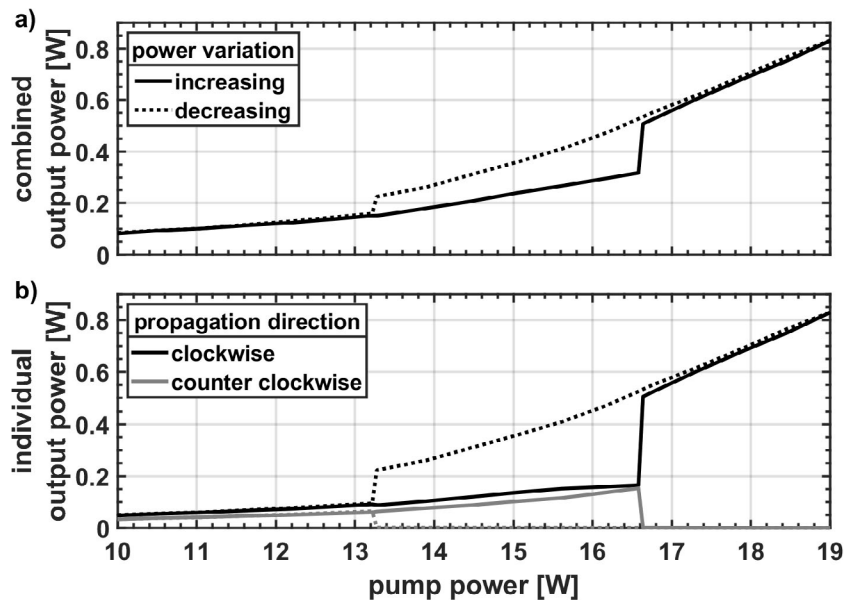


**Figure 7.** Evolution of (a) the combined and (b) the individual output power with respect to the propagation directions for the third ring cavity with low output coupling ratio and 2 km passive fiber demonstrating a bistability and unidirectional lasing behavior.

The individual power evolution of both propagation directions is distinguished in figure 7(b)). While increasing the pump power both propagation directions operate at nearly the same output power up to 16.3 W pump power where the combined output power switches to a higher level, as discussed above. After this point the powers propagating in the two directions differ significantly. The output power of the clockwise direction roughly triples whereas the output power of the counter clockwise direction nearly shuts off to just a few mW. We expect this residual few mW output power to originate from the high power clockwise direction by internal cavity reflections at splices and due to Rayleigh scattering in the 2 km long passive fiber.

While decreasing the pump power the output in the counter propagating direction remains close to zero far below the initial switching point down to the pump power of 13.3 W where

both propagation directions switch back to a similar power. The hysteresis visible in the combined power is clearly visible in the individual power behaviors, as well.

Within the accuracy of our pump diode supply current of 0.1 A, which correlates to a change in pump power of 60 mW, the observed behavior appears to be a sudden switch rather than a gradual transition for both switching points. This behavior was repeatable for weeks with minor changes in the switching pump power  $< 0.5$  W presumably due to changes in the environmental conditions.

The spectral evolution of the clockwise direction output during increase of pump power is displayed in figure 8. Prior to the nonlinear switching at 16.3 W pump power up to 5 broadened Stokes peaks are visible, superimposed by a very complex spectral fine structure similar to the first, 1 km-cavity layout. After the nonlinear switching a 6nd Stokes peak

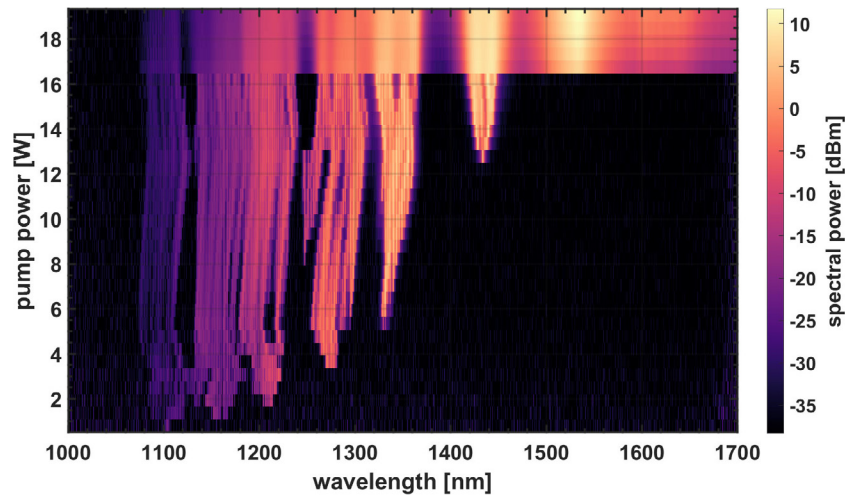


**Figure 8.** Spectral evolution of the clockwise direction output during increase of pump power for the third ring cavity with low output coupling fraction and 2 km passive fiber.

appears accompanied by a broad background up to the analyzers wavelengths limit of 1700 nm. Interestingly, the complex fine structure has vanished and the entire spectrum now has a very smooth envelope. The spectral gaps which remain around 1250 nm and 1380 nm again originate from elevated propagation losses in the 2 km long passive fiber due to O–H absorption.

#### 4. Discussion and conclusion

We demonstrated a new way of generating a continuous wave supercontinuum pumped at 1  $\mu\text{m}$  wavelengths using an all-fiber ring cavity and utilizing among others simulated Stokes Raman scattering. It appears that the kind of dispersion, whether it is normal or anomalous, does not have an impact on the broadening mechanism. Unaffected by the zero dispersion wavelength of the passive fiber HI1060 around 1400 nm the evolution and appearance of the spectrum is consistent through the entire spectral range from 1100 nm up to 1700 nm. This implies that the contributing nonlinear effects are identical which is in contrast to [14, 15]. Therein, a twofold spectral distribution is demonstrated with individual Stokes peaks appearing only in the normal dispersion range and a flat and continuous generation of new wavelengths components in the anomalous dispersion range. In consequence our approach seems not to rely on anomalous dispersion and basically any single mode step index fiber can be used.

Stimulating the Stokes Raman scattering in a ring cavity with a small output coupling ratio employs the following benefits. First, the onset of stimulated Stokes Raman scattering is strongly shifted to smaller powers by the strong self-seeding mechanism and it is relatively easy to excite several Stokes orders and cover a broad spectral range. Second, additional nonlinear effects are triggered by the strong feedback resulting in strongly broadened and finally connected Stokes peaks constituting a SC instead of separated Stokes peaks.

Third, the envelope of the output spectrum is strongly defined by the wavelengths dependency of the output coupler.

Hence, an adapted output coupler can specifically address the spectral needs of a given application and keep unrequired optical power within the cavity to further spur nonlinear effects and wavelength generation.

Finally, we demonstrated the previously unobserved phenomenon of optical bistability and isolator-free unidirectional lasing in an all-fiber ring laser, using a simple all-fiber setup designed for high nonlinearities. While at low pump power similar output power is emitted in both clockwise and counter clockwise direction, situation changes after a given power threshold where the laser emits light in only one direction. In addition, switching on and off of one propagation direction happens at different pump power levels leading to a distinct hysteresis behavior.

The observed phenomenon is an interesting nonlinear optical effect which opens new possibilities and points to attractive applications. As such it definitely deserves further discussion and investigation. Future work will focus on revealing the contributing nonlinear effects which lead to the broadening and merging of the Stokes peaks and finally to the optical bistability and isolator-free unidirectional lasing phenomenon described here.

#### References

- [1] Dudley J M and Taylor J R (ed) 2010 *Supercontinuum Generation in Optical Fibers* (Cambridge: Cambridge University Press)
- [2] Itoh H, Davis G M and Sudo S 1989 *Opt. Lett.* **14** 1368
- [3] Mussot A, Lantz E, Maillotte H, Sylvestre T, Finot C and Pitois S 2004 *Opt. Express* **12** 2838
- [4] Gordon J P 1986 *Opt. Lett.* **11** 662
- [5] Dianov E M, Karasik A I, Mamyshev P V, Prokhorov A M, Serkin V N, Stel'makh M F and Fomichev A A 1985 *JETP Lett.* **41** 294
- [6] Korneev N, Kuzin E A, Ibarra-Escamilla B, Bello-Jiménez M and Flores-Rosas A 2008 *Opt. Express* **16** 2636
- [7] Islam M N, Sucha G, Bar-Joseph I, Wegener M, Gordon J P and Chemla D S 1989 *Opt. Lett.* **14** 370
- [8] Popov S V, Taylor J R, Rulkov A B and Gapontsev V P 2004 *Conf. Lasers Electro-Optics* p CThEE4

- [9] Avdokhin A V, Popov S V and Taylor J R 2003 *Opt. Lett.* **28** 1353
- [10] Bloembergen N 1967 *Am. J. Phys.* **35** 989
- [11] Stolen R H, Ippen E P and Tynes A R 1972 *Appl. Phys. Lett.* **20** 62
- [12] Abraham E and Smith S D 1982 *Rep. Prog. Phys.* **45** 815
- [13] Jalas D et al 2013 *Nat. Photon.* **7** 579
- [14] Kobtsev S M and Kukarin S V 2010 *Laser Phys.* **20** 372
- [15] Lei C, Song R, Yao J and Hou J 2017 *Proc. SPIE 4th Int. Symp. Laser Interaction with Matter* **10173** 101731Z